

Design and Electrical Performance Analysis of AlGaAs/InGaAs/InP Pseudomorphic HEMT

M V Ganeswara Rao, N. Ramanjaneyulu, Y. Madhu Sudhana Reddy, Neravati Nagaraja Kumar, Palle Rangappa, M. Chennakesavulu

Abstract—In this paper, the computer-aided simulation-based design and performance analysis of a type of low-noise and high-frequency AlGaAs/InGaAs/InP pseudomorphic HEMT optimized with a recessed gate structure are reported. The variation of gate and drain voltages has been studied in detail for the influence on critical DC and electrical parameters such as ON current (I_{on}), OFF current (I_{off}), and ratio I_{on}/I_{off} . The HEMT was demonstrated to have excellent electric performances. I_{on} reaches 0.397 mA, and I_{off} is as low as $1.72E-16$ A at $V_{ds} = 2$ V. It has a very impressive ratio of I_{on}/I_{off} that is much better than any HEMT architectures already reported. In this work, GaAs, AlGaAs, and InGaAs material system was used to provide the semiconductor structure for a device that had high electron mobility along with increased switching speeds that have become critical for high frequency operation. Using machine learning models, delta doping regions were optimized both above and below the InGaAs channel so that the electron flow was maintained under tight control. Such parameters have been achieved with the highest achievable potential and electric field values of 2.65 V and $7.19E4$ V/cm, respectively, significantly contributing to better confinement and performance of the electrons in the channel. In this work, other electrical parameters such as transconductance (g_m)-the value of which was 0.2 mS-and the maximum drain current (I_{dss})-0.39 A-have also been discussed. The performance of the proposed pseudomorphic HEMT clearly indicates its feasibility in low-noise, high-frequency mobile and satellite communication applications where conventional transistor-based technologies cannot compete for purely reasons of efficiency and reliability.

Index Terms—Delta doping, HEMT, pseudomorphic, InGaAs, potential

I. INTRODUCTION

The modern electronics sector is in great demand to develop high-frequency applications in RFICs and wireless communication systems. Advanced semiconductor de-

vices are required to sustain this advanced technology [1]. Traditional metal-oxide-semiconductor field-effect transistors (MOSFETs) face great challenges while being scaled down to nanometer dimensions due to higher leakage currents and reduced performance [2]. These limitations have prompted researchers to explore alternative transistor architectures capable of maintaining high performance, low power consumption, and low noise in such applications. High Electron Mobility Transistors (HEMTs) have emerged as a robust alternative, offering superior electron mobility and velocity, which are critical for applications requiring high-frequency operation, such as satellite and mobile communications [3,4,5].

Especially pseudomorphic HEMTs (pHEMTs), HEMTs are favored over the traditional semiconductor with the ability to overcome that semiconductor's limitation. pHEMT takes advantage of composite materials with different lattice constants that introduce strain into the device's structure so that it is possible to develop a two-dimensional electron gas (2DEG) in the channel [6,7,8,9]. This 2DEG could provide greatly improved electron mobility, which would be an important feature for increasing switching speed, lowering power consumption, and sustaining high-frequency response. These characteristics make pHEMTs ideal for a variety of applications, including millimeter-wave communication, radar systems, and RF amplifiers [10].

The materials employed in pHEMTs, such as Gallium Arsenide (GaAs), Aluminum Gallium Arsenide (AlGaAs), and Indium Gallium Arsenide (InGaAs), are carefully chosen for their complementary properties [11]. GaAs serves as the substrate and provides a low-resistance path for current flow, while the AlGaAs layer acts as a barrier, preventing electrons from leaking in undesired directions. Here, due to its better electron mobility, the conduction-channel is provided by InGaAs, which itself leads to the formation of the 2DEG [12,13,14]. The unique combination of these materials leads to outstanding high-frequency performance, and as a result, pHEMTs are a viable solution for low-noise, high-power applications [15].

In this study, we explore the design and performance characteristics of a pseudomorphic HEMT with a recessed gate structure, optimized for low-noise, high-frequency applications [16]. The device is based on a GaAs substrate with an InGaAs channel sandwiched between two AlGaAs regions. The novelty of this design lies in the use of delta doping—regions of concentrated dopants placed strategically above and below the InGaAs channel—to enhance the flow of electrons [17,18,19]. The delta doped regions enhance the electron concentration in

Manuscript received September 29, 2024; revised January 3, 2025.

M V Ganeswara Rao is an Associate Professor of Department of Electronics and Communication Engineering, Shri Vishnu Engineering College for Women, Bhimavaram, India. (e-mail: ganesh.mgr@gmail.com).

N. Ramanjaneyulu is an Associate Professor of Department of ECE, Rajeev Gandhi Memorial College of Engineering and Technology, Nandyal, A.P, India. (e-mail: rams9ganguly@gmail.com).

Y.Madhu Sudhana Reddy is an Associate Professor of Department of ECE, Rajeev Gandhi Memorial College of Engineering and Technology, Nandyal, A.P, India. (e-mail: ymsr1016@gmail.com).

Neravati Nagaraja Kumar is an Associate Professor of Department of ECE, Rajeev Gandhi Memorial College of Engineering and Technology, Nandyal, A.P, India. (e-mail: rajuneravati@gmail.com).

Palle Rangappa is an Assistant Professor of Department of ECE, Rajeev Gandhi Memorial College of Engineering and Technology, Nandyal, A.P, India. (e-mail: palleranga.476@gmail.com).

M. Chennakesavulu is an Associate Professor of Department of ECE, Rajeev Gandhi Memorial College of Engineering and Technology, Nandyal, A.P, India. (e-mail: chennakesava318@gmail.com).

TABLE I
PROPOSED DEVICE DESIGN PARAMETERS

Device parameter	Value
Gate length	0.5 μm
Channel length	4.5 μm
Source, drain length	1 μm
Spacer length	0.5 μm
Thickness of AlGaAs above InGaAs	30 nm
Thickness of AlGaAs below InGaAs	40 nm
Thickness of InGaAs	20 nm
Workfunction of gate	4.55 eV
Mobility of electrons	12000 $\text{cm}^2/\text{V} - \text{s}$
Mobility of holes	2000 $\text{cm}^2/\text{V} - \text{s}$
Velocity saturation in the channel	2×10^7
Concentration of GaAs	$2 \times 10^{18} \text{ cm}^{-3}$
Concentration of AlGaAs	$5 \times 10^{15} \text{ cm}^{-3}$
Concentration of Delta doping in AlGaAs	$8 \times 10^{18} \text{ cm}^{-3}$
Concentration of spacer AlGaAs	$5 \times 10^{15} \text{ cm}^{-3}$
Carrier lifetime of electrons	1×10^{-8}
Carrier lifetime of holes	1×10^{-8}

the channel; thus, the electrical properties are improved, for example, higher I_{on}/I_{off} ratio, better transconductance (g_m), and lower power consumption [20,21]. The pseudomorphic HEMT design discussed in the present work is, above all, especially suitable for high frequencies and low noise levels. It, therefore, attracts some kind of solution to the challenges in modern RF and communication technologies. Compared to conventionally designed MOSFETs and other types of HEMTs, it outweighs them clearly in terms of speed and efficiency as well as noise suppression [22]. As the properties of material are further optimized together with the architecture of a device, pHEMTs will soon be part and parcel of future wireless and satellite communication systems [23,24]. It talks about the proposed pHEMT in a very elaborate manner of its structure and electrical performance and a basis for further evolution of high-frequency semiconductor devices.

II. STRUCTURE OF PROPOSED DEVICE

The proposed Pseudomorphic HEMT with a recessed gate is shown in Figure 1. It consists of composite materials AlGaAs, InGaAs, and InP. The composition of Al and Ga in AlGaAs is 0.22 and 0.78 respectively. The design parameters used the proposed device are tabulated in Table. I. The channel length of 4.5 μm is chosen in a structure with a gate length of 0.5 μm . The other two terminals of HEMT namely the source and the drain are chosen to be 1 μm . The proposed device consists of a double channel that uses 2 delta dopings. Both the delta dopings are chosen below and above the channel in both the AlGaAs regions. The thickness of these models is chosen to be 10 angstrom. The planar concentration (expressed in cm^{-2}) delta doping must be accounted for bulk doping (expressed in cm^{-3}) taking the thickness across layers. GaAs materials are chosen to formulate the source and the drain capacitor regions. Two different doping distributions are used namely the Gaussian and the complementary error function under the heavily doped source and drain regions.

The width of AlGaAs consisting of one delta doping above InGaAs is taken as 30 nm and the width of AlGaAs consisting of other delta doping below InGaAs is chosen to be 40 nm. The width of the InGaAs layer is taken to be 20 nm. The concentration of InGaAs is chosen as $5 \times 10^{15} \text{ cm}^{-3}$. Different models are taken into account to analyze the behavior of electrons in the device. Shockley-Read-Hall recombination model and electric field-dependent mobility models are used to analyze this behavior. The mobility of electrons and holes is taken as 12000 $\text{cm}^2/\text{V} - \text{s}$ and 2000 $\text{cm}^2/\text{V} - \text{s}$ respectively. Other models like conmob and fldmob are chosen to analyze the mobility of electrons/holes in the conduction state and flat band state. The workfunction of the gate is taken to be 4.55 eV. The concentration of GaAs is $2 \times 10^{18} \text{ cm}^{-3}$ whereas the concentration of AlGaAs is $5 \times 10^{15} \text{ cm}^{-3}$. The delta doping used in the structure has AlGaAs as the material with a concentration of $8 \times 10^{18} \text{ cm}^{-3}$. The spacer used between the source/drain and gate has $5 \times 10^{15} \text{ cm}^{-3}$ with AlGaAs material.

For hetero materials used in the design like GaAs and AlGaAs, the corresponding regions are characterized by doping-dependent mobilities and lifetimes of electrons and holes. The recombination lifetimes of electrons and holes are taken as 1×10^{-8} and 1×10^{-8} respectively. The velocity saturation of electrons and holes is chosen as 2×10^7 to have the carrier transport of the device. In the case of the InGaAs region of the device, the carrier lifetime of the device is deliberately used while defining the material statements of the device. The alignment of energy bands in the channel region is explicitly defined by suitable parameters,

III. RESULTS AND DISCUSSION

Figure 2 shows the energy band diagram of the proposed device with different biasing conditions. The energy band diagram shows the variation of conduction band energy and valence band energy across the length of the channel. To have a clear understanding, initially, the device energy bands are shown in the OFF state ($V_{ds} = 0\text{V}$, $V_{gs} = 0\text{V}$). In the OFF state, the electrons in the source side do not have enough potential to move to the drain side. To have the current flow, the movement of electrons should take place and this is not predominant in the OFF state. In the process of analysis, the gate is kept at 0V and the drain voltage is increased to 2V. In this case, the electrons are made possible to move but as the gate voltage is not present, the channel is not formed and hence the electrons do not move. The gate voltage is made to vary from -4V, -2V, -1.5V by keeping the drain voltage at 2V. We can observe that as the gate voltage is varied the energy bands have come closer making it possible for electrons to penetrate from the band.

The transfer I-V characteristics are important to analyze the behavior of the device. The ON current, and OFF current of the device are determined by the drain current obtained by varying the gate voltage. Figure 3 shows the transfer characteristics of the device at $V_{ds}=2\text{V}$. The gate voltage is swept from -1.5V to 0V. The drain current characteristics are needed to understand the behavior of the device for applied drain voltages. Figure 4

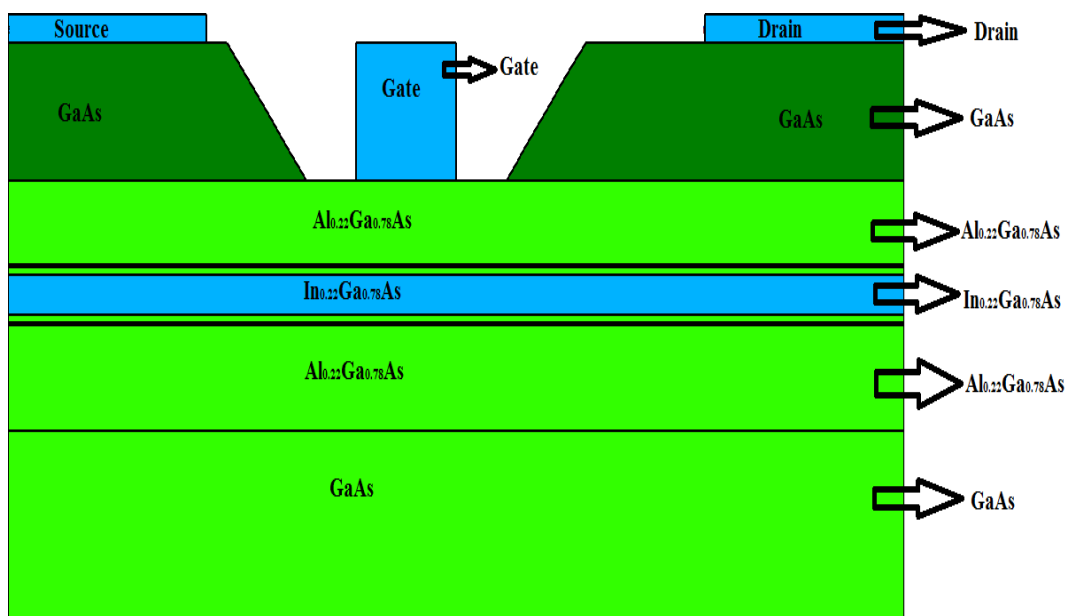


Fig. 1. Structure of Proposed device

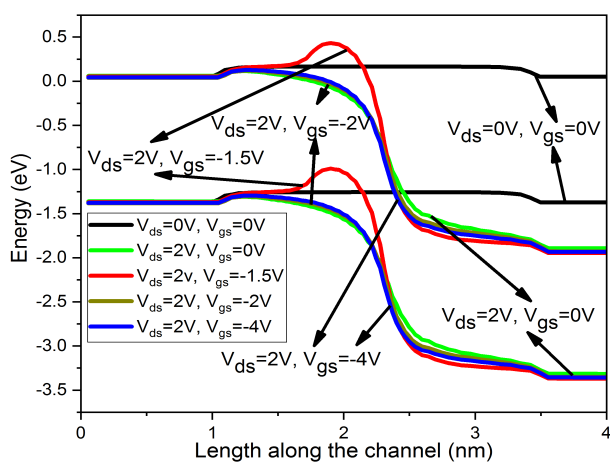


Fig. 2. Energy band across the channel

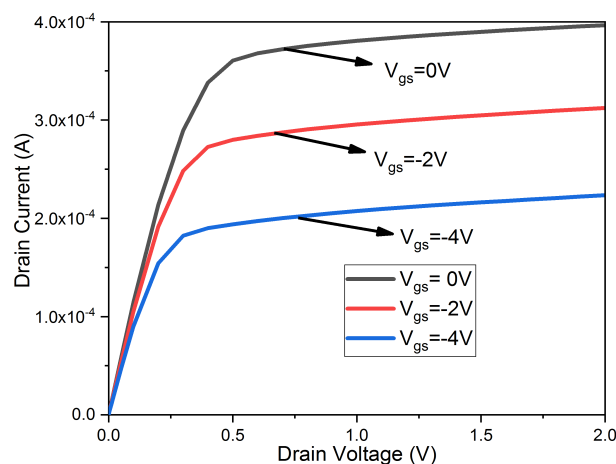


Fig. 4. $I_d - V_{ds}$ characteristics for $V_{gs}=1V$

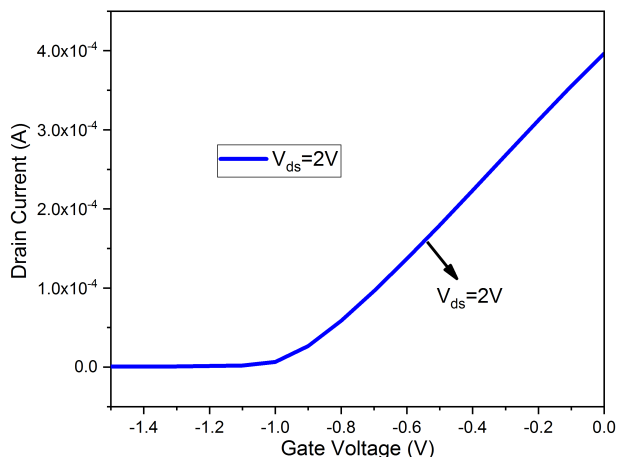


Fig. 3. $I_d - V_{gs}$ characteristics for $V_{ds}=1V$

shows the drain current characteristics by varying drain voltage from 0V to 2V for a fixed gate voltage at 0V, -2V, and -4V. It can be observed from Figure 4 that the drain current is increased by increasing gate voltage. The operation region of the device is at linear region and saturation region.

The potential distribution of the device across the channel is an important electrical performance parameter to analyze the electron concentration in the device. It is a key parameter that shows the behavior of charge carriers responsible for electrical properties of the device. It is evident that the potential distribution is not uniform throughout the length of the channel. Different regions of the device are taken with different concentrations of either p-type or n-type. Also, the potential distribution is affected by the doping profile across regions, the structure of the device, and the voltage of operation. Figure 5 shows the potential distribution which is not of much interest. It can be seen that a higher concentration of

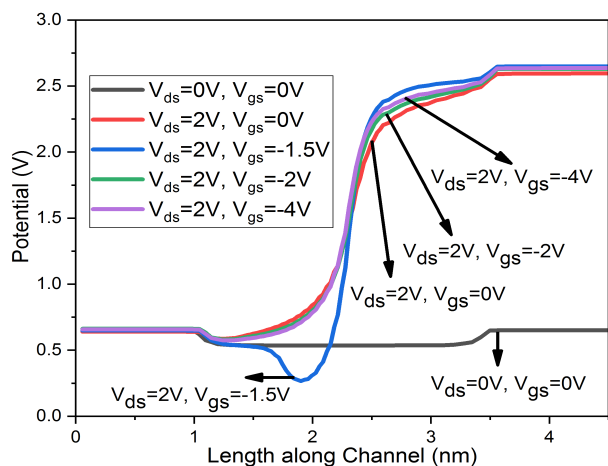


Fig. 5. Proposed device Potential distribution

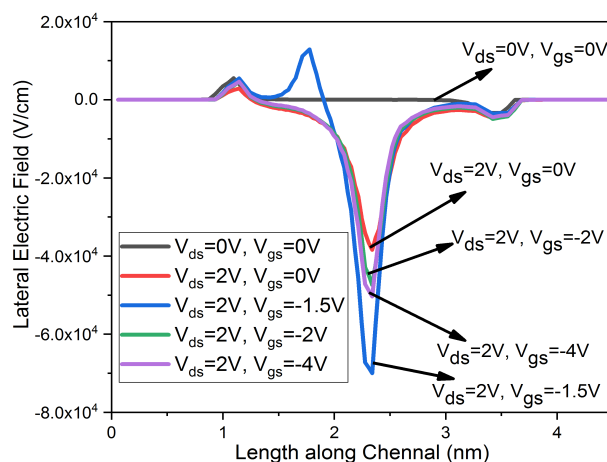


Fig. 7. Proposed device Lateral electric field distribution

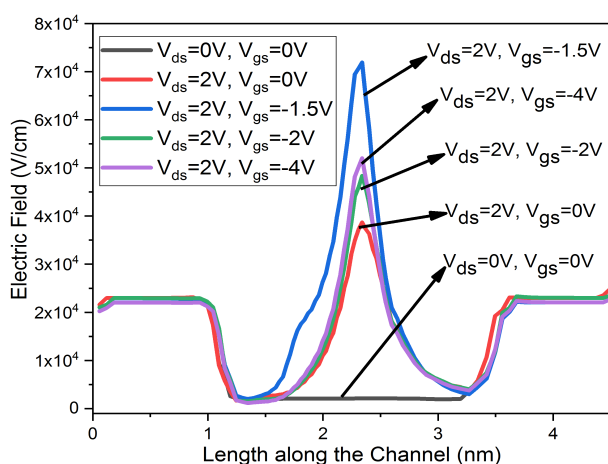


Fig. 6. Proposed device Electric field distribution

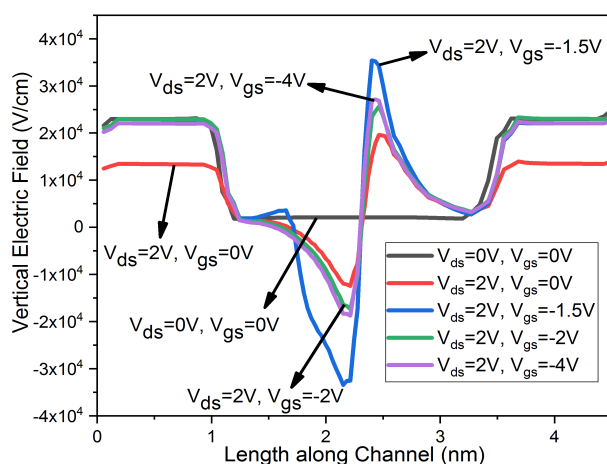


Fig. 8. Proposed device Transverse electrical field distribution

potential distribution is seen with higher gate voltage. The potential distribution can be controlled to have enhanced speed of operation and minimum noise operation.

The potential analysis also concentrates on the electric field distribution in the device. It can be seen from Figure 6 that the electric field plays a crucial role in HEMT simulations. The OFF-state electric field does not have any significant impact, while the electric field at the channel has tremendously increased by giving a suitable gate voltage. The electric field lines impinge from gate to drain, gate to source. As the recessed pseudomorphic HEMT has a spacer between the recessed gate and source/drain, the electric field in that region is zero as it does not have any impact on device operation. The same can also be seen in Figure 6 where the net electric field is zero in the spacer region and it keeps increasing exactly at the channel region.

The lateral electric field distribution is shown in Figure 7. The potential distribution between two terminals of the device is the key factor in generating a lateral electric field. In general, the lateral electric field is not uniform throughout the device for a given biasing voltage. From Figure 7, the OFF state lateral electric field is almost zero because there is no

potential difference between the gate and source/drain. As the p-n junction is formed at the gate channel region, the lateral electric field is stronger near the p-n junctions that are formed. Also, Figure 7 shows a sharp rise in the lateral electric field because of an abrupt change in doping concentration.

The transverse electric field significantly influences the semiconductor device operation. The flow of charge carriers is controlled by this electric field which in turn influences the overall performance of the device. Several device parameters impact the strength of the transverse electric field like the concentration of dopants, structure of device, and operating voltage. This transverse electric field influences the movement of electrons perpendicular to the direction of the electric field. The strength is directly proportional to the applied gate voltage. It can be seen from Figure 8 that the perpendicular electric field is spread asymmetrically in the channel. This asymmetric behavior is mainly because of transverse electric field behavior causing it to spread across the channel. Significantly high perpendicular electric field is observed at greater gate voltage. Table. II shows the comparison of the performance parameters of the proposed device with existing HEMT architectures.

Figure 9 shows the spatial variation of electron concentra-

TABLE II
COMPARISON OF PERFORMANCE PARAMETERS OF PROPOSED HEMT WITH EXISTING ARCHITECTURES

Parameter	[12]	[13]	[14]	[15]	Proposed Structure
I_{on} (mA)	0.32	0.37	0.365	0.372	0.397
I_{off} (A)	0.5E-14	1.2E-14	1.8E-15	1.8E-15	1.72E-16
I_{on}/I_{off}	A	B	C	D	E
$C_{gs,max}$ (F)	0.8E-12	0.9E-14	-	-	1.4E-15
V_t (V)	-	-	1.2	0.6	-0.9
$g_{m,max}$ (mS)	0.42	0.64	-	0.72	0.2
I_{dss} (A)	0.65	0.47	0.6	0.8	0.39
$Potential_{max}$ (V)	1.2	1.39	2.01	2.4	2.65
E_{max} (V/cm)	6.5E3	6.89E4	6.3E4	-	7.19E4
$E_{x,max}$ (V/cm)	-	-	-	-	1.29E4
$E_{y,max}$ (V/cm)	-	-	-	-	3.54E4

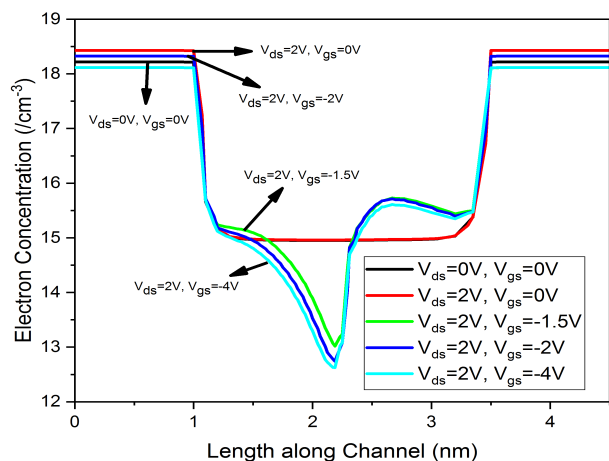


Fig. 9. Proposed device Electron concentration distribution across channel

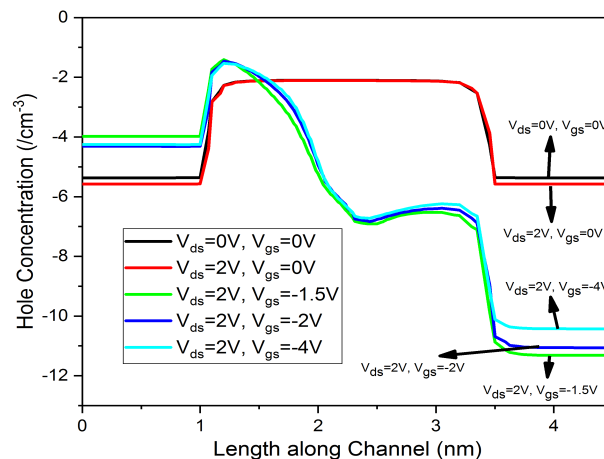


Fig. 10. Proposed device Hole concentration distribution across channel

tion along the channel of a pseudomorphic High Electron Mobility Transistor, pHEMT. Maximum electron concentration is seen inside the InGaAs channel forming a two-dimensional electron gas. This 2DEG is an important characteristic of the pHEMT device structure, which ensures that electrons move with high mobility and the device performance can be improved. The electron concentration is sharply peaked within this channel due to the confinement created by the heterostructure's design. Moving away from the channel towards the source and drain regions, the electron concentration decreases, which indicates a less pronounced influence of the gate potential in these areas.

It is because of the careful engineering of the device's channel and doping profiles that distinct characteristics in the electron distribution arise. Delta doping located both above and below the InGaAs channel is one such critical source of increasing electron density. The highly doped regions are strong enough to confine electrons within the channel, resulting in a dense population of electrons. This confinement is critical for the formation of the 2DEG, thereby enhancing the overall conductivity and performance of the device. Material properties also determine the electron concentration distribution. The combination of GaAs, AlGaAs, and InGaAs materials is crucial for achieving high electron mobility and effective confinement. Differences in bandgaps among these materials create potential wells that attract and hold electrons within the

channel. In addition, the gate voltage modulates the electron concentration by controlling the potential barrier at the gate-channel interface. The higher gate voltage confinement of electrons releases a sharp peak in the electron concentration.

Figure 10 shows the hole concentration distribution in the channel of the pseudomorphic High Electron Mobility Transistor (pHEMT). In contrast to electrons, holes play a relatively minor role in the conduction process in pHEMTs. This is because pHEMTs are designed to make use of the high electron mobility within the two-dimensional electron gas (2DEG). The figure shows that the hole concentration is much smaller throughout the channel and has variations mainly dependent on material composition and device structure. The peak hole concentration occurs near the source and drain regions where p-n junctions are formed, and then drops rapidly within the channel where the electron concentration is dominant.

Several factors contribute to the hole concentration characteristics in this device. The delta doping of InGaAs above and below the channel enhances electron confinement while reducing hole concentration in the channel region. The design maintains the channel to be electron-rich, which limits hole participation in the conduction process. The heterostructure of the materials, GaAs, AlGaAs, and InGaAs, contributes to this distribution. The band alignment between these materials results in creating a potential barrier that limits hole accumu-

lation in the channel.

IV. CONCLUSION

The impact of the gate and the drain voltage on DC and electrical parameters of pseudomorphic HEMT for low noise application is discussed in detail. DC parameters are improved to a greater extent which concentrates more on the switching characteristics of the device. An ON current of 0.397 mA for $V_{ds}=2$ V is obtained for the proposed structure. Machine learning models used to induce delta doping above and below InGaAs layers have shown the possibility for higher performance. Suitable high values of potential and electric field are achieved. The I_{on}/I_{off} also improved significantly than other existing HEMT architectures. All the discussed parameters are within permissible range for low-noise applications.

REFERENCES

- [1] Chabak KD, Walker DE, Johnson MR, Crespo A, Dabiran AM, Smith DJ, Wowchak AM, Tetlak SK, Kossler M, Gillespie JK, Fitch RC, Trejo M (2011) High-performance AlN/GaN HEMTs on sapphire substrate with an oxidized gate insulator. *IEEE Electron Device Lett* 32(12):1677–1679.
- [2] Mishra, U.K., Parikh, P., Wu, Y.F.: AlGaIn/GaN HEMTs—an overview of device operation and applications. *Proc. IEEE* 90, 1022–1031 (2002)
- [3] B. Naresh Kumar Reddy, M.H.Vasanth and Y.B.Nithin Kumar, “A Gracefully Degrading and Energy-Efficient Fault Tolerant NoC Using Spare core”, 2016 IEEE Computer Society Annual Symposium on VLSI, pp. 146-151, 2016.
- [4] Chiu, H.C., Liu, C.H., Huang, C.R., Chiu, C.C., Wang, H.C., Kao, H.L., Lin, S.Y., Chien, F.T.: Normally-of p-GaN gated AlGaIn/ GaN MIS-HEMTs with ALD-grown Al₂O₃/AlN composite gate insulator. *Membranes* 11, 727 (2021)
- [5] Arivazhagan, L., Nirmal, D., Godfrey, D., Ajayan, J., Prajoun, P., Augustine Fletcher, A.S., Amir Anton Jone, A., Raj Kumar, J.S.: Improved RF and DC performance in AlGaIn/GaN HEMT by P-type doping in GaN bufer for millimetre-wave applications. *Int. J. Electron. Commun. (AEÜ)* 108, 189–194 (2019)
- [6] Huang, S., Wang, X.H., Liu, X.Y., Sun, Q., Chen, K.J.: An ultrathin-barrier AlGaIn/GaN heterostructure: a recess-free technology for the fabrication and integration of GaN-based power devices and power-driven circuits. *Semicond. Sci. Technol.* 36, 044002 (2021)
- [7] B. Naresh Kumar Reddy “Design and implementation of high performance and area efficient square architecture using Vedic Mathematics,” *Analog Integr Circ Sig Process*, 2019.
- [8] Wu, H., Fu, X.J., Wang, Y., Guo, J.W., Shen, J.Y., Hu, S.D.: Breakdown voltage improvement of enhancement mode AlGaIn/ GaN HEMT by a novel step-etched GaN bufer structure. *Results Phys.* 29, 104768 (2021)
- [9] Tallarico, A.N., Stofels, S., Posthuma, N., Bakeroot, B., Decoutere, S., Sangiorgi, E., Fiegna, C.: Gate reliability of p-GaN HEMT with gate metal retraction. *IEEE Trans. Electron. Dev.* 66, 4829–4835 (2019)
- [10] Hosseinzadeh Sani, M., Khosroabadi, S.: Improving thermal effects and reduction of self-heating phenomenon in AlGaIn/ GaN/Si based HEMT. *J. Electron. Mater.* 50, 2295–2304 (2021)
- [11] B. Naresh Kumar Reddy, MZU Rahman, A Lay-Ekuakille, “Enhancing Reliability and Energy Efficiency in Many-Core Processors Through Fault-Tolerant Network-On-Chip,” *IEEE Transactions on Network and Service Management*, 2024.
- [12] Kuzmik, J., Javorka, P., Alam, A., Marso, M., Heuken, M., Kordos, P.: Investigation of self-heating effects in AlGaIn-GaN HEMTs. In: 2001 International Symposium on Electron Devices for Microwave and Optoelectronic Applications. EDMO 2001 (Cat. No. 01TH8567) (pp. 21–26). *IEEE* (2001)
- [13] Cozette, F., et al.: Resistive nickel temperature sensor integrated into short-gate length AlGaIn/GaN HEMT dedicated to RF applications. *IEEE Electron Device Lett.* 39(10), 1560–1563 (2018)
- [14] Menozzi, R., Umana-Membreno, G.A., Nener, B.D., Parish, G., Sozzi, G., Faraone, L., Mishra, U.K.: Temperature-dependent characterization of AlGaIn/GaN HEMTs: thermal and source/ drain resistances. *IEEE Trans. Device Mater. Reliab.* 8(2), 255– 264 (2008)
- [15] Padmanabhan, B., Vasileska, D., Goodnick, S.M.: Is selfheating responsible for the current collapse in GaN HEMTs *J. Comput. Electron.* 11, 129–136 (2012)
- [16] Simms, R.J., Pomeroy, J.W., Uren, M.J., Martin, T., Kuball, M.: Channel temperature determination in high-power AlGaIn/GaN HFETs using electrical methods and Raman spectroscopy. *IEEE Trans. Electron Devices* 55(2), 478–482 (2008)
- [17] Rodríguez, R., González, B., García, J., Yigletu, F.M., Tirado, J.M., Iniguez, B., Nunez, A.: Numerical simulation and compact modelling of AlGaIn/GaN HEMTs with mitigation of self-heating effects by substrate materials. *Phys Status Sol(a)*. 212(5), 1130– 1136 (2015)
- [18] Sadi, T., Kelsall, R.W., Pilgrim, N.J., et al.: Monte Carlo study of self-heating in nanoscale devices. *J. Comput. Electron.* 11, 118–128 (2012)
- [19] Gu. Yan, D. Chang, H. Sun, J. Zhao, G. Yang, Z. Dai, Yu. Ding, *Electronics* 8, 885 (2019)
- [20] S. Rahman, N.A.F. Othman, S.W.M. Hatta, N. Soin, *ECS J. SolidState Sci. Technol.* 6(12), P805 (2017)
- [21] Rao, M. G., Ramanjaneyulu, N., Pydi, B., Soma, U., Babu, K. R., & Prasad, S. H. (2023). Enhancing performance of dual-gate FinFET with high-K gate dielectric materials in 5 nm technology: a simulation study. *Transactions on Electrical and Electronic Materials*, 24(6), 557-569.
- [22] K. Raghava Rao, Md Zia Ur Rahman, Krishna Prasad Satamraju and B Naresh Kumar Reddy, “Genetic Algorithm for Cross-Layer based Energy Hole Minimization in Wireless Sensor Networks,” *IEEE Sensors Letters*, Vol. 06, 2022.
- [23] J. Petterson, M. Edoif, C. Platzer-Björkman, Electrical modeling of Cu(In, Ga)Se₂ cells with ALD-Zn1-xMgxO bufer layers. *J. Appl. Phys.* 111, 014509 (2012).
- [24] A. Gueddim, N. Bouarissa, Theoretical investigation of the conduction and valence band ofsets of GaAs1-xNx/GaAs1-yNy heterointerfaces. *Appl. Surf. Sci.* 253(17), 7336–7341 (2007).